

Communication

## Kinetic Isotope Effect of Prostaglandin H Synthase Exhibits Inverted Temperature Dependence

Gang Wu \*, Richard J. Kulmacz and Ah-Lim Tsai

Department of Internal Medicine, University of Texas Medical School at Houston, 6431 Fannin St., Houston, TX 77030, USA; E-Mails: richard.j.kulmacz@uth.tmc.edu (R.J.K.); ah-lim.tsai@uth.tmc.edu (A.-L.T.)

\* Author to whom correspondence should be addressed; E-Mail: gang.wu@uth.tmc.edu; Tel.: +713-500-6802; Fax: +713-500-6812.

Received: 28 February 2014; in revised form: 24 April 2014 / Accepted: 23 May 2014 /

Published: 11 June 2014

---

**Abstract:** Conversion of arachidonic acid to prostaglandin G<sub>2</sub>/H<sub>2</sub> catalyzed by prostaglandin H synthase (PGHS) is proposed to involve initial transfer of the C13 pro-(S) hydrogen atom from arachidonate to the Tyr385 radical in PGHS, followed by insertion of two oxygen molecules and several chemical bond rearrangements. The initial hydrogen-transfer was recently concluded to be a rate-limiting step in cyclooxygenase catalysis based on the observed intrinsic deuterium kinetic isotope effect values ( $^Dk_{cat}$ ). In the present study, we have found that  $^Dk_{cat}$  values of both PGHS-1 and -2 show an unusual increase with temperatures in the range of 288–310 K, exhibiting an inverted temperature dependence. The value of  $\ln^Dk_{cat}$ , however, decreased linearly with  $1/T$ , consistent with a typical Arrhenius relationship.

**Keywords:** prostaglandin H synthase-1 and -2; deuterium kinetic isotope effect; temperature dependence of KIE

---

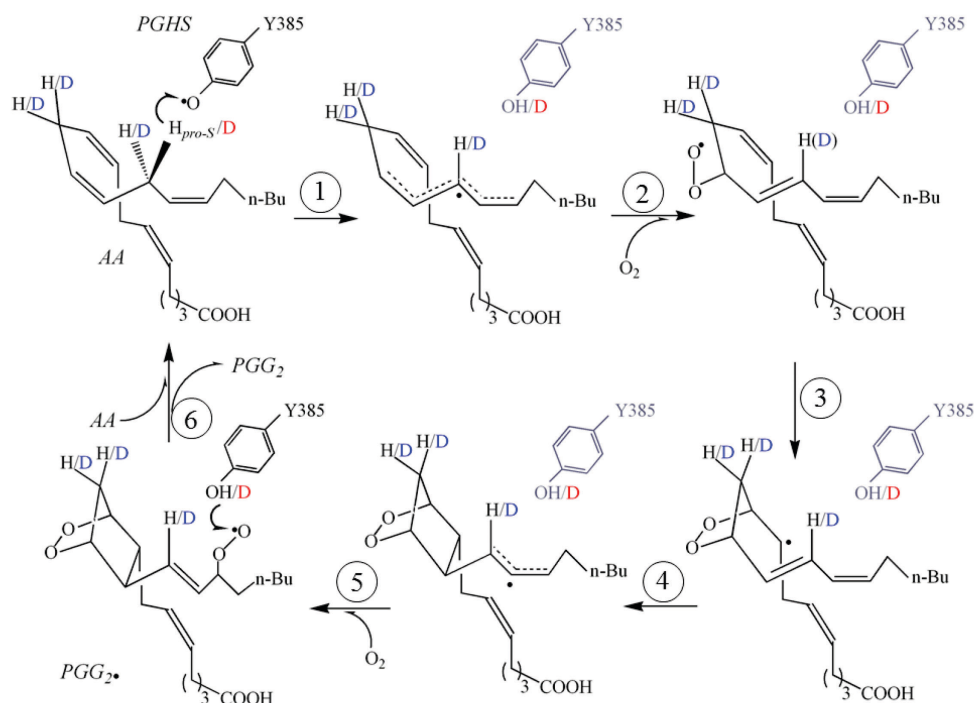
### 1. Introduction

Prostaglandin H synthase (PGHS) catalyzes the biosynthesis of prostaglandin H<sub>2</sub> (PGH<sub>2</sub>), which is the precursor of all the prostaglandins, thromboxanes and prostacyclins [1,2]. There are two isoforms, PGHS-1 and PGHS-2, each having both peroxidase and cyclooxygenase activities [1]. PGHS reacts with peroxide at its peroxidase site to generate Intermediate I, which contains a ferryl heme and

a proto-porphyrin radical; subsequent intra-molecular electron transfer from an adjacent tyrosine residue to the ferryl heme yields Intermediate II and a tyrosine radical [3–5]. This tyrosyl radical is the starting point of cyclooxygenase catalysis, which transforms arachidonic acid (AA) to prostaglandin G<sub>2</sub> (PGG<sub>2</sub>) [6,7]. PGG<sub>2</sub> is itself a peroxide, and can be reduced to PGH<sub>2</sub> by the peroxidase activity of PGHS.

The tyrosyl radical mechanism of cyclooxygenase catalysis (Scheme 1) is consistent with most of the experimental evidence [4,6,8]. In this mechanism, the cyclooxygenase reaction starts with the abstraction of the C13 pro-(*S*) hydrogen of AA by a tyrosyl radical located on Tyr385 in PGHS-1 (Tyr371 in PGHS-2) (step 1). This hydrogen abstraction generates an AA pentadienyl radical with spin density distributed over C11–C15. Insertion of O<sub>2</sub> at C11 generates a peroxy radical intermediate (step 2) that next forms an endoperoxide across C11 and C9 and leaves the radical at C8 (step 3). Subsequent cyclization between C8 and C12 forms a cyclopentane ring and a delocalized radical over C13–C15 (step 4). The insertion of a second O<sub>2</sub> at C15 produces a PGG<sub>2</sub> radical (step 5), which then abstracts the hydroxyl hydrogen from Tyr385 to produce PGG<sub>2</sub> and regenerate the Tyr385 radical (step 6). Finally, PGG<sub>2</sub> dissociates from the cyclooxygenase catalytic site and leaves PGHS ready for the next cyclooxygenase cycle [8].

**Scheme 1.** Hypothetical mechanism for PGHS-1 and -2 cyclooxygenase catalysis [9] using AA or d<sub>4</sub>-AA as substrate. Deuterium substitutions are labeled with “D”. Deuterium substitution at the pro-(*S*) hydrogen at C13 of AA gives the primary kinetic isotope effect (KIE) and is labeled in red; other deuterium substitutions are labeled in blue. The reversibility of individual reaction steps has not been established, so all are depicted as irreversible. Tyrosine 385 may not participate in the O<sub>2</sub> insertion and AA double bond rearrangement steps and so this residue is shown in lighter color. Tyrosine 385 in PGHS-1 corresponds to tyrosine 371 in PGHS-2.



Kinetic isotope effect (KIE) studies have been used to characterize the cyclooxygenase mechanism [9–12]. In an early experiment, observations of isotope enrichment in the unreacted substrate after PGHS incubations with tritium-substituted 8,11,14-eicosatrienoic acid indicated that the initial hydrogen abstraction from the substrate (step 1, Scheme 1) is rate-limiting in PGHS cyclooxygenase catalysis [9]. Recently, the KIE of the hydrogen abstraction step in PGHS-1 was measured directly using AA and 13,13-d<sub>2</sub>-AA with rapid-freeze quenching EPR and computer modeling methods [10]. The resulting KIE value for hydrogen abstraction was small,  $^Dk (=k_H/k_D) = 1.9\text{--}2.3$ , but comparable to the steady-state noncompetitive KIE values observed for PGHS-1 and -2 using the same protio and deutero AAs,  $^Dk_{\text{cat}} (k_{\text{cat,H}}/k_{\text{cat,D}}) = 1.8\text{--}2.3$  [10]. The similarity of the KIE values determined using the different methods is consistent with the initial hydrogen abstraction step being a rate-limiting step in cyclooxygenase catalysis [10]. Interestingly, results from a study of competitive O<sup>18</sup> isotope effects in PGHS-1 indicated that formation of the endoperoxide ring or the bicyclic intermediate (steps 3 and 4, Scheme 1) may be irreversible [11].

Recent KIE studies using perdeuterated linoleic acid (d<sub>31</sub>-LA) as the substrate instead of deuterated AA reported much larger  $^Dk_{\text{cat}}$  values, >30 for PGHS-1 and >22 for PGHS-2 [12]. This presumed substrate-dependence of KIE was not observed in lipoxygenases (LOX)—a family of fatty acid oxygenases that oxidize LA-AA and other fatty acid substrates by inserting a hydroperoxy group into the fatty acid chains [13,14]. LOX catalysis is thought to start with a rate-limiting hydrogen abstraction from the fatty acid by a non-heme ferric center, Fe<sup>3+</sup>-OH [15]. Soybean LOX exhibits large deuterium KIEs for both LA, 18–80 [15–18] and AA, 97 [19], attributed to significant hydrogen tunneling in both substrates [20].

In addition to the magnitude of KIEs, information on the temperature dependence of KIEs can also provide important insight into the mechanisms [21]. Most theoretical models based on transition state theory or hydrogen tunneling predict smaller activation energy for hydrogen than deuterium and therefore a reciprocal correlation between KIE and temperature, called a normal temperature dependence [21,22]. This normal temperature dependence has been observed in many enzymes [21]. The KIE for PGHS-2 with d<sub>31</sub>-LA has been shown to decrease slightly with increasing temperature [12]. In the present study, we found that the activation energies for PGHS-1 or -2 with 10,10,13,13-d<sub>4</sub>-AA (d<sub>4</sub>-AA) are smaller than that for PGHS-1 or -2 with AA and therefore KIEs for PGHS increase with the temperature, showing abnormal, or inverted, temperature dependence. There are only a few reported examples of KIE values increasing with temperature in chemical reactions [23–27] and enzymatic catalyses [16,28].

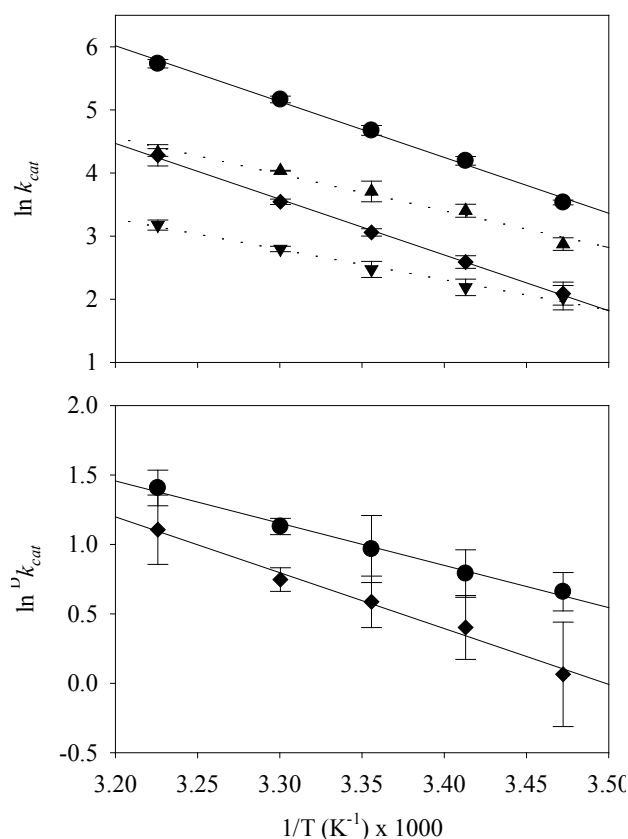
## 2. Results and Discussion

The catalytic rate constants of PGHS-1 and -2 cyclooxygenase activities were calculated from their measured maximum O<sub>2</sub> consumption rates ( $v_{\text{opt}}$ ) in reactions at pH 7.2 with saturating levels of AA or d<sub>4</sub>-AA [10]. The resulting  $k_{\text{cat}}$  values at temperatures of 288–310 K are listed in Table 1. With AA, the  $k_{\text{cat}}$  value of PGHS-1 increased from 34.2 s<sup>-1</sup> at 288 K to 308.6 s<sup>-1</sup> at 310 K, and the  $k_{\text{cat}}$  of PGHS-2 increased from 17.7 to 75.6 s<sup>-1</sup> over the same temperature range. With d<sub>4</sub>-AA, the corresponding  $k_{\text{cat}}$  values ranged from 8.1–72.3 s<sup>-1</sup> for PGHS-1 and 7.6–23.9 s<sup>-1</sup> for PGHS-2, respectively.

**Table 1.** Effects of temperature on  $k_{\text{cat}}$  and  $^{\text{D}}k_{\text{cat}}$  of PGHS. Turnover numbers and primary KIE values,  $^{\text{D}}k_{\text{cat}}$ , are shown for PGHS-1 and -2 at the indicated temperatures and pH 7.2. The values shown are averages  $\pm$  standard deviation ( $N = 4$ ).

Temp. K	PGHS-1			PGHS-2		
	$k_{\text{catAA}}, \text{S}^{-1}$	$k_{\text{catd4-AA}}, \text{S}^{-1}$	$^{\text{D}}k_{\text{cat}}$	$k_{\text{catAA}}, \text{S}^{-1}$	$k_{\text{catd4-AA}}, \text{S}^{-1}$	$^{\text{D}}k_{\text{cat}}$
288	$34.2 \pm 1.3$	$17.7 \pm 1.8$	$1.9 \pm 0.3$	$8.1 \pm 1.8$	$7.6 \pm 1.5$	$1.1 \pm 0.4$
293	$66.2 \pm 4.5$	$30.1 \pm 3.1$	$2.2 \pm 0.4$	$13.3 \pm 3.1$	$8.9 \pm 1.2$	$1.5 \pm 0.3$
298	$107.3 \pm 8.3$	$40.8 \pm 6.7$	$2.6 \pm 0.6$	$21.3 \pm 6.7$	$11.9 \pm 1.5$	$1.8 \pm 0.3$
303	$175.1 \pm 9.2$	$56.6 \pm 0.3$	$3.1 \pm 0.2$	$34.6 \pm 0.3$	$16.4 \pm 0.7$	$2.1 \pm 0.2$
310	$308.6 \pm 20.7$	$75.6 \pm 4.6$	$4.1 \pm 0.5$	$72.3 \pm 4.6$	$23.9 \pm 1.9$	$3.0 \pm 0.8$

**Figure 1.** Temperature dependence of PGHS cyclooxygenase activity and deuterium KIE. **Upper panel:** The logarithm of  $k_{\text{cat}}$  is plotted as a function of reciprocal temperature. Circles, PGHS-1/AA; diamonds, PGHS-2/AA; triangles, PGHS-1/d<sub>4</sub>-AA; inverted triangles, PGHS-2/d<sub>4</sub>-AA. Solid lines: linear fit for reactions using AA; dashed lines: linear regression for reactions using d<sub>4</sub>-AA; **Lower panel:** The logarithm of deuterium KIE ( $^{\text{D}}k_{\text{cat}}$ ) is plotted as a function of reciprocal temperature. Circles: PGHS-1; diamonds: PGHS-2. Lines: linear regression. Error bars represent standard deviations ( $N = 4$ ).



The value of  $\ln k_{\text{cat}}$  exhibited a linear dependence on the reciprocal of absolute temperature for both isozymes and both substrates (Figure 1, upper panel). This result indicated that the activation energies for cyclooxygenase catalysis by PGHS-1 and -2 remained unchanged over the experimental temperature range. This behavior is in line with the previous mechanistic studies of PGHS-1 and -2 [9,10]. The

temperature dependence of  $k_{\text{cat}}$  on  $1/T$  fits well with the empirical Arrhenius equation,  $k_{\text{cat}} = A e^{-E_a/RT}$ , where  $A$  is the Arrhenius prefactor,  $E_a$  is the activation energy and  $R$  is the gas constant. The fitted  $E_a$  and  $A$  parameters for PGHS-1 and -2 are summarized in Table 2. With AA as the substrate, the activation energies of PGHS-1 and -2 were essentially identical—74 and 73 kJ/mol, respectively (Table 2). With  $d_4$ -AA, the  $E_a$  of PGHS-1 was 48 kJ/mol, ~20% higher than the  $E_a$  of PGHS-2 (40 kJ/mol) (Table 2). The Arrhenius prefactors for PGHS-1,  $7.9 \times 10^{14} \text{ s}^{-1}$  for AA and  $1.1 \times 10^{10} \text{ s}^{-1}$  for  $d_4$ -AA, were significantly larger than those for PGHS-2,  $1.6 \times 10^{14} \text{ s}^{-1}$  for AA and  $1.3 \times 10^8 \text{ s}^{-1}$  for  $d_4$ -AA (Table 2). The much larger prefactors for PGHS-1 clearly account for most of the difference in overall cyclooxygenase activities between PGHS-1 than -2 seen in Table 1.

**Table 2.** Activation parameters of PGHS-1 and -2.

	$E_{a,H}$ (kJ·mol <sup>-1</sup> )	$E_{a,D}$ (kJ·mol <sup>-1</sup> )	$\Delta E_a$ (kJ·mol <sup>-1</sup> )	$A_H$ (s <sup>-1</sup> )	$A_D$ (s <sup>-1</sup> )	$A_H/A_D$
PGHS-1/AA <sup>a</sup>	74	48	25	$7.9 \times 10^{14}$	$1.1 \times 10^{10}$	$7.9 \times 10^4$
PGHS-2/AA <sup>a</sup>	73	40	33	$1.6 \times 10^{14}$	$1.3 \times 10^8$	$1.2 \times 10^6$
PGHS-2/LA <sup>b</sup>			0.04			20
Soybean LOX/LA <sup>c</sup>	8.8		3.8	$9 \times 10^3$		18

<sup>a</sup> The parameters were obtained by fitting the  $\ln k_{\text{cat}}$  vs.  $1/T$  data at 288–310 K with AA as the substrate;  $\Delta E_a = E_{a,H} - E_{a,D}$ ; <sup>b</sup> [11]; <sup>c</sup> [18].

The activation energies obtained by fitting to the Arrhenius relationship (Figure 1A) presumably include a non-enzymatic contribution reflecting the temperature-dependent permeability of the O<sub>2</sub> electrode membrane. The permeability of this membrane, made of Teflon, has a temperature coefficient of 3%–5% per degree [29]. This corresponds to an apparent energy term of 17–25 kJ/mol (Figure S1). Since the same type of O<sub>2</sub> electrode membrane material was used for all cyclooxygenase measurements, the energy term due to the membrane permeability was the same regardless of the enzyme or substrate used. Subtracting the energy term for the membrane permeability, the corrected activation energies of the cyclooxygenase catalysis with AA were 49–57 kJ/mol for PGHS-1 and 48–56 kJ/mol for PGHS-2. The corrected activation energy of PGHS-1 approximately agreed with a quantum mechanics calculation for the cyclooxygenase reactions of PGHS-1 [30]. On the other hand, the calculated  $\Delta E_a$  values in Table 2 do not need correction for membrane permeability because this contribution to the energy cancels.

The observation of similar activation energies for PGHS-1 and -2 using a given substrate suggests that the two isozymes have similar transition states in the rate-determining step(s) of the cyclooxygenase reactions with each substrate. The difference between the prefactors of PGHS-1 and -2 may be related to the structural difference in the substrate binding sites and catalytic dynamics in these two isozymes [5,31,32]. For both PGHS-1 and -2, deuterium substitution at C10 and C13 of AA markedly decreased the activation energy, from 74 to 48 kJ/mol in PGHS-1 and from 73 to 40 kJ/mol in PGHS-2, respectively (Table 2). This observation is surprising because deuterium substitution generally decreases the zero point energy in a reactant more than in a transition state, and thus increases the activation energy [21,33]. Deuterium substitution of AA also resulted in much smaller prefactor values, from  $7.9 \times 10^{14}$  to  $1.1 \times 10^{10} \text{ s}^{-1}$  for PGHS-1 and from  $1.6 \times 10^{14}$  to  $1.3 \times 10^8 \text{ s}^{-1}$  in PGHS-2, resulting in very large  $A_H/A_D$  ratios,  $7.9 \times 10^4$  for PGHS-1 and  $1.2 \times 10^6$  for PGHS-2

(Table 2). Combining the kinetic parameters (Table 1) and activation parameters (Table 2) of PGHS-1 and -2, PGHS-1 and -2 exhibited small  $^Dk_{\text{cat}}$ 's whose magnitude increased with temperature, namely an inverted or abnormal dependence on temperature (Table 1 and Figure 1, lower panel).

In contrast to the small  $^Dk_{\text{cat}}$ 's observed for PGHS-1 and -2 with AA (Table 1),  $^Dk_{\text{cat}}$ 's for PGHS-1 and -2 oxygenation reactions with LA have been found to be large, in the range of 22–30 [12]. Moreover, the activation energy of PGHS-2 with  $d_{31}$ -LA was just  $\sim 0.04$  kJ/mol higher than with LA [12] and the  $A_H/A_D$  ratio was 20 [12], which is significant but very much smaller than that observed for PGHS-2 with AA in the present study (Table 2). Therefore,  $^Dk_{\text{cat}}$  of PGHS-2 with LA decreased slightly with temperature [12]. Overall, the activation parameters for PGHS with LA were comparable with those of soybean LOX with the same fatty acid (Table 2) [18].

The KIEs of most chemical reactions and enzymatic catalyses exhibit normal temperature dependence; namely they decrease with increased temperature [21]. The normal temperature dependence of KIE has been explained successfully by many theoretical analyses. On the other hand, only a few examples of KIE increasing with reaction temperature have been published. The non-enzymatic reactions include: (1) the dehydrohalogenation of certain halogen substituted ethylbenzenes [23]; (2) the addition reaction of *m*-nitro- $\beta,\beta$ -difluorostyrene [24]; (3) the reaction between ubiquinol-10 and 5,7-diisopropyltocopheroxyl radical [25]; (4) the proton-coupled electron-transfer (PCET) from ubiquinol to  $\text{Ru}(\text{bpy})_2(\text{pbim})^+$  ( $\text{bpy} = 2,2'$ -dipyridyl;  $\text{pbim} = 2$ -(2-pyridyl)-benzimidazolate) [27]; and (5) the hydride transfer from 5-methyl-6-phenyl-5,6-dihydrophenanthridine (G-PDH) substituted with electron-donating groups to thioxanthylum ( $\text{TX}^+$ ) [26]. All these chemical reactions were conducted in alcohol or acetonitrile. We are aware of only two examples of enzymatic catalysis where the KIE increased with temperature. In an early study, the KIE of soybean LOX purified from dry soybeans with LA were found to increase from 18 at 273 K to 60 at 305 K; slight decreases were seen at higher temperatures [16]. However, for recombinant soybean LOX expressed in *E. coli*, the KIE with LA was reported to decrease with temperature [15]. The second example of an enzyme KIE with inverted temperature dependence is human platelet 12-lipoxygenase (*h*12-LOX) using  $d_4$ -AA as the substrate [28].

Explaining inverted temperature dependence in a KIE is a challenging task and only a few theoretical treatments for single step chemical reactions are available [22,26]. Theoretical analysis of the PCET from ubiquinol to  $\text{Ru}(\text{bpy})_2(\text{pbim})^+$  indicated that a KIE of inverted temperature dependence in a PCET reaction may arise in a system with proton donor-acceptor motion of high frequency and small inner-space and solvent reorganization energies [22]. In such a system, when the 0/0 pair of reactant/product vibronic states is in the inverted Marcus region while the 0/1 pair of reactant/product vibronic states is in the normal Marcus region and is the dominant contributor to the overall rate, the free energy barrier is lower for deuterium, giving an increase in KIE with temperature [22]. A theoretical approach based on thermodynamics and kinetics analyses was used to explain the inverted temperature dependence of the KIE for the hydride transfer from G-PDH to  $\text{TX}^+$  [26]. In this case, it was proposed that the hydride transfer from G-PDH to  $\text{TX}^+$  occurs via a two-stage mechanism with two elementary chemical steps: (1) the two reactants approach each other to reversibly form a charge transfer complex that accomplishes partial electron transfer without chemical bond formation or breakage; and (2) hydrogen bearing a partial negative charge transfers irreversibly from the G-PDH-moiety to the  $\text{TX}$ -moiety [26]. In this case, it was demonstrated that both normal and inverted temperature-dependence

of deuterium KIE could be observed in a single reaction. For G-PDH substituted with electron-withdrawing groups, the second step is not favored and the H<sup>-</sup> transfer exhibits a KIE of normal temperature dependence. For G-PDH substituted with electron-donating groups, the second step is favored and the H<sup>-</sup> transfer exhibits a KIE of inverted temperature dependence [26]. There is as yet no detailed theoretical analysis for the hydrogen transfer from AA to Tyr385 radical in PGHS; it remains to be seen whether either of these theoretical analyses mentioned above is relevant to the inverted temperature dependence of the KIEs observed in reactions of PGHS-1 and -2 with AA.

Catalysis by enzymes usually involves multiple reaction steps and the observed KIE reflects the interplay of the kinetics of several steps, both isotope-sensitive and isotope-insensitive. The KIE being observed may differ from the intrinsic KIE of the isotope sensitive step(s), especially when such a step(s) is not rate-limiting under the conditions used, due to the kinetic complexity caused by the other steps. For soybean LOX purified from dry soybeans, the increase of KIE with temperature (up to 305 K) was attributed to a temperature-dependent change in the rate-limiting step(s) [16]. It was shown that the hydrogen abstraction from LA by Fe<sup>3+</sup>-OH becomes rate-limiting above 305 K, where the KIE is large and almost temperature independent [15,16]. The increase of KIE with temperature for oxygenation of AA by h12-LOX was also attributed to a shift of rate-limiting step(s) [28].

Although cyclooxygenase catalysis also begins with hydrogen abstraction from a fatty acid substrate, PGHS utilizes a tyrosyl radical as the oxidant in place of the Fe<sup>3+</sup>-OH used by LOX (Scheme 1). At room temperature and with excess O<sub>2</sub>, abstraction of the C13 pro-(S) hydrogen from AA or LA by the Tyr385 radical (step 1) is likely the rate-limiting step in PGHS oxygenation reactions [9,10,12]. Compared to the large KIE for PGHS-2 reacted with LA [12], the KIEs for PGHS-1 and -2 with AA are quite small but very similar to the intrinsic KIE for hydrogen abstraction from AA by PGHS-1 [10]. It is possible that the intrinsic KIE is obscured at lower temperatures and revealed better at higher temperatures as the hydrogen abstraction step becomes more rate-limiting (Figure 1, lower panel). However, the small sizes of KIEs of PGHS-1 and -2 with AA at the highest experimental temperature (≤4.1, Table 1) and the good linear relationship between  $\ln k_{\text{cat}}$  and  $1/T$  seem to argue against a change in the rate-limiting step(s) as the explanation for the observed increase in KIE with temperature.

The KIE for PGHS-2 reacted with LA exhibited only a weak but normal temperature dependence [12]. The significant difference in the magnitude of KIEs of PGHS with AA and LA was attributed to the discrepancies in the interactions between AA and LA and the cyclooxygenase active site [12]. Mutations in the active site of soybean LOX were shown to result in different catalytic dynamics in the oxygenation of LA, leading to KIEs of different temperature dependence [18]. In PGHS, the wide variation in cyclooxygenase  $K_M$  values among different fatty acid substrates indicates substrate-dependent interactions with the active site [34,35]. These substrate-dependent interactions are also revealed by the crystal structures of PGHS with fatty acids such as AA, LA,  $\alpha$ -linolenic acid, eicosapentaenoic acid and docosahexaenoic acid [31,36,37]. Such discrepancy in interactions between cyclooxygenase active site and various fatty acid substrates likely lead to different catalytic dynamics and transition states in the oxygenations of various fatty acids by PGHS, exhibiting KIEs of different magnitude and temperature dependence. Further detailed investigations of active site dynamics with different fatty acids may improve understanding of KIEs and mechanism(s) for PGHS cyclooxygenase catalysis.

PGHS catalysis plays the pivotal role in the syntheses of all prostanoids. The dependence of PGHS catalysis on temperature likely affects the controls of many physiological processes at different temperatures. In humans, although the core body temperature is maintained around 37 °C, it does fluctuate under different states, such as after exercises. Body temperature may also be different at peripheral tissues. More significant changes in body temperature happen under pathological conditions such as inflammation. Understanding the temperature dependence of PGHS catalysis will provide insights into how many physiological processes are affected by the change in body temperature and will also provide guidelines on administering antipyretic drugs, many of which are inhibitors of PGHS. Moreover, the different temperature dependence of PGHS and LOX catalysis presumably affects the relative ratios between prostanoids, HpETEs and leukotrienes under different temperatures since these hormones are synthesized from AA in humans by PGHS and LOX, respectively [38,39].

### 3. Experimental Section

#### 3.1. Materials

Hemin was purchased from Sigma (St. Louis, MO, USA) or Porphyrin Products (Logan, UT, USA). Tween 20 was from Anatrace (Maumee, OH, USA). Arachidonic acid was purchased from Nu-Chek Prep, Inc. (Elysian, MN, USA). The 10,10,13,13-d<sub>4</sub>-AA was synthesized with high purity by total synthesis as reported before [40,41].

PGHS-1 was purified as the apoenzyme from ram seminal vesicles [42] and human PGHS-2 was purified as a recombinant protein overexpressed in baculovirus-infected insect cells [43]. The PGHS-1 and -2 holoenzymes were reconstituted as previously described [44]. The concentrations of PGHS-1 and -2 holoenzymes were calculated based on their A<sub>410</sub> using an extinction coefficient of 165 mM<sup>-1</sup>·cm<sup>-1</sup> [45]. The cyclooxygenase specific activities of individual PGHS preparations were determined under standard conditions at 30 °C with a YSI Model 5331 electrode, covered by a Standard membrane (YSI #5793) and a YSI Model 53 monitor (Yellow Springs Instrument Co., Yellow Springs, OH, USA) [45]. Reactions were conducted in 3 mL of 0.1 M potassium phosphate buffer, pH 7.2 containing 1 mM phenol, 100 μM AA and 0.05% Tween 20. The optimal cyclooxygenase velocity ( $v_{opt}$ ) for each reaction was calculated from the slope of a tangent to the steepest part of the recorded [O<sub>2</sub>] vs. time plot. The  $k_{cat}$  ( $v_{opt}/[PGHS]$ ) for AA consumption under these standard conditions was typically  $\geq 100$  s<sup>-1</sup> for purified PGHS-1 and  $\geq 15$  s<sup>-1</sup> for purified PGHS-2 (assuming 2 mol O<sub>2</sub> consumed per mol AA).

#### 3.2. Measurement of Non-Competitive Kinetic Isotope Effect

The noncompetitive steady-state KIE was calculated as the ratio of AA conversion rates (determined from O<sub>2</sub> consumption) with AA and d<sub>4</sub>-AA as the substrate. The enzyme concentration was 11 nM for PGHS-1 and 13 nM for PGHS-2. The working stocks of AA and d<sub>4</sub>-AA were prepared by evaporating the organic solvent with a stream of N<sub>2</sub> gas, adding suitable volume of 0.1 M Tris, pH 8.5 buffer, and vortexing to achieve a homogeneous suspension. The concentrations of the substrate stock solutions were determined from the extents of O<sub>2</sub> consumption in reactions with limiting fatty acid and excess O<sub>2</sub> and PGHS-1, assuming that 2 mol O<sub>2</sub> are consumed per mol AA. For measurements

of KIE, the concentrations of AA and d<sub>4</sub>-AA were 60–70 μM, essentially saturating given the K<sub>M</sub>'s of PGHS-1 and -2 for the substrates [10]. Under these v<sub>max</sub> conditions, k<sub>cat</sub> could be calculated by dividing the observed cyclooxygenase velocity by the PGHS concentration (k<sub>cat</sub> = v<sub>max</sub>/[PGHS]). The primary KIE, <sup>D</sup>k<sub>cat</sub>, was calculated as <sup>D</sup>k<sub>cat</sub> = k<sub>cat,H</sub>/k<sub>cat,D</sub>.

For temperature dependence experiments, the cyclooxygenase reaction temperature was controlled at 15–37 °C by a Fisher Scientific Isotemp model 3016 water bath (Fisher Scientific, Pittsburgh, PA, USA), which has a temperature stability of ±0.01 °C. In these experiments, the oxygen electrode was covered by a High Sensitivity membrane (YSI #5794), which has a higher O<sub>2</sub> permeability than the Standard membrane and responds more quickly to changes in [O<sub>2</sub>]. Increases in cyclooxygenase KIE with reaction temperature were also observed in tests using the Standard membrane (data not shown), so the electrode response characteristics were not an issue in reliable KIE measurements.

#### 4. Conclusions

The kinetic isotope effect for PGHS cyclooxygenase catalysis exhibits an inverted temperature dependence. Theoretical interpretation of this phenomenon will provide important insight into the mechanism of PGHS.

#### Acknowledgments

We thank Wilfred A. van der Donk, Department of Chemistry, University of Illinois at Urbana-Champaign, for kindly providing the 10,10,13,13-d<sub>4</sub>-AA. This work was supported by NIH grant R01 HL095820 to Ah-Lim Tsai.

#### Conflicts of Interest

The authors declare no conflict of interest.

#### References

1. Smith, W.L.; Garavito, R.M.; DeWitt, D.L. Prostaglandin endoperoxide H synthases (cyclooxygenases)-1 and -2. *J. Biol. Chem.* **1996**, *271*, 33157–33160.
2. Samuelsson, B.; Goldyne, M.; Granstrom, E.; Hamberg, M.; Hammarstrom, S.; Malmsten, C. Prostaglandins and thromboxanes. *Annu. Rev. Biochem.* **1978**, *47*, 997–1029.
3. Shimokawa, T.; Kulmacz, R.J.; Dewitt, D.L.; Smith, W.L. Tyrosine-385 of prostaglandin endoperoxide synthase is required for cyclooxygenase catalysis. *J. Biol. Chem.* **1990**, *265*, 20073–20076.
4. Tsai, A.-L.; Kulmacz, R.J. Tyrosyl radicals in prostaglandin H synthase-1 and-2. *Prostaglandins Other Lipid Mediat.* **2000**, *62*, 231–254.
5. Kiefer, J.R.; Pawlitz, J.L.; Moreland, K.T.; Stegeman, R.A.; Hood, W.F.; Gierse, J.K.; Stevens, A.M.; Goodwin, D.C.; Rowlinson, S.W.; Marnett, L.J.; *et al.* Structural insights into the stereochemistry of the cyclooxygenase reaction. *Nature* **2000**, *405*, 97–101.
6. Tsai, A.-L.; Kulmacz, R.J. Prostaglandin H synthase: Resolved and unresolved mechanistic issues. *Arch. Biochem. Biophys.* **2010**, *493*, 103–124.

7. Rouzer, C.A.; Marnett, L.J. Mechanism of free radical oxygenation of polyunsaturated fatty acids by cyclooxygenases. *Chem. Rev.* **2003**, *103*, 2239–2304.
8. Van der Donk, W.A.; Tsai, A.-L.; Kulmacz, R.J. The cyclooxygenase reaction mechanism. *Biochemistry* **2002**, *41*, 15451–15458.
9. Hamberg, M.; Samuelsson, B. On the mechanism of the biosynthesis of prostaglandins E-1 and F-1- $\alpha$ . *J. Biol. Chem.* **1967**, *242*, 5336–5343.
10. Wu, G.; Lu, J.M.; van der Donk, W.A.; Kulmacz, R.J.; Tsai, A.-L. Cyclooxygenase reaction mechanism of prostaglandin H synthase from deuterium kinetic isotope effects. *J. Inorg. Biochem.* **2011**, *105*, 382–390.
11. Mukherjee, A.; Brinkley, D.W.; Chang, K.M.; Roth, J.P. Molecular oxygen dependent steps in fatty acid oxidation by cyclooxygenase-1. *Biochemistry* **2007**, *46*, 3975–3989.
12. Danish, H.H.; Doncheva, I.S.; Roth, J.P. Hydrogen tunneling steps in cyclooxygenase-2 catalysis. *J. Am. Chem. Soc.* **2011**, *133*, 15846–15849.
13. Andreou, A.; Feussner, I. Lipoxygenases—Structure and reaction mechanism. *Phytochemistry* **2009**, *70*, 1504–1510.
14. Prigge, S.T.; Boyington, J.C.; Faig, M.; Doctor, K.S.; Gaffney, B.J.; Amzel, L.M. Structure and mechanism of lipoxygenases. *Biochimie* **1997**, *79*, 629–636.
15. Rickert, K.W.; Klinman, J.P. Nature of hydrogen transfer in soybean lipoxygenase 1: Separation of primary and secondary isotope effects. *Biochemistry* **1999**, *38*, 12218–12228.
16. Glickman, M.H.; Klinman, J.P. Nature of rate-limiting steps in the soybean lipoxygenase-1 reaction. *Biochemistry* **1995**, *34*, 14077–14092.
17. Glickman, M.H.; Klinman, J.P. Lipoxygenase reaction mechanism: Demonstration that hydrogen abstraction from substrate precedes dioxygen binding during catalytic turnover. *Biochemistry* **1996**, *35*, 12882–12892.
18. Knapp, M.J.; Rickert, K.; Klinman, J.P. Temperature-dependent isotope effects in soybean lipoxygenase-1: Correlating hydrogen tunneling with protein dynamics. *J. Am. Chem. Soc.* **2002**, *124*, 3865–3874.
19. Peng, S.; van der Donk, W.A. An unusual isotope effect on substrate inhibition in the oxidation of arachidonic acid by lipoxygenase. *J. Am. Chem. Soc.* **2003**, *125*, 8988–8989.
20. Jonsson, T.; Glickman, M.H.; Sun, S.J.; Klinman, J.P. Experimental evidence for extensive tunneling of hydrogen in the lipoxygenase reaction: Implications for enzyme catalysis. *J. Am. Chem. Soc.* **1996**, *118*, 10319–10320.
21. Pu, J.; Gao, J.; Truhlar, D.G. Multidimensional tunneling, recrossing, and the transmission coefficient for enzymatic reactions. *Chem. Rev.* **2006**, *106*, 3140–3169.
22. Ludlow, M.K.; Soudackov, A.V.; Hammes-Schiffer, S. Theoretical analysis of the unusual temperature dependence of the kinetic isotope effect in quinol oxidation. *J. Am. Chem. Soc.* **2009**, *131*, 7094–7102.
23. Koch, H.F.; Dahlberg, D.B.; McEntee, M.F.; Klecha, C.J. Use of kinetic isotope effects in mechanism studies. Anomalous arrhenius parameters in the study of elimination reactions. *J. Am. Chem. Soc.* **1976**, *98*, 1060–1061.
24. Koch, H.F.; Koch, A.S. Proton-transfer reactions. 5. An observed primary kinetic isotope effect that increases with increasing temperature. *J. Am. Chem. Soc.* **1984**, *106*, 4536–4539.

25. Nagaoka, S.; Nishioku, Y.; Mukai, K. Tunneling effect in the regeneration reaction of vitamin E by ubiquinol. *Chem. Phys. Lett.* **1998**, *287*, 70–74.
26. Zhu, X.Q.; Li, X.T.; Han, S.H.; Mei, L.R. Conversion and origin of normal and abnormal temperature dependences of kinetic isotope effect in hydride transfer reactions. *J. Org. Chem.* **2012**, *77*, 4774–4783.
27. Cape, J.L.; Bowman, M.K.; Kramer, D.M. Reaction intermediates of quinol oxidation in a photoactivatable system that mimics electron transfer in the cytochrome bc1 complex. *J. Am. Chem. Soc.* **2005**, *127*, 4208–4215.
28. Wecksler, A.T.; Jacquot, C.; van der Donk, W.A.; Holman, T.R. Mechanistic investigations of human reticulocyte 15- and platelet 12-lipoxygenases with arachidonic acid. *Biochemistry* **2009**, *48*, 6259–6267.
29. Yellow Springs Instrument Co. *Instructions for YSI Model 53 Biological Oxygen Monitor*; Yellow Springs Instrument Co.: Yellow Springs, OH, USA, 1987.
30. Blomberg, L.M.; Blomberg, M.R.A.; Siegbahn, P.E.M.; van der Donk, W.A.; Tsai, A.L. A quantum chemical study of the synthesis of prostaglandin G<sub>2</sub> by the cyclooxygenase active site in prostaglandin endoperoxide H synthase 1. *J. Phys. Chem. B* **2003**, *107*, 3297–3308.
31. Malkowski, M.G.; Ginell, S.L.; Smith, W.L.; Garavito, R.M. The productive conformation of arachidonic acid bound to prostaglandin synthase. *Science* **2000**, *289*, 1933–1937.
32. Garavito, R.M.; Mulichak, A.M. The structure of mammalian cyclooxygenases. *Annu. Rev. Biophys. Biomol. Struct.* **2003**, *32*, 183–206.
33. Simon, H.; Palm, D. Isotope effects in organic chemistry and biochemistry. *Angew. Chem. Int. Ed.* **1966**, *5*, 920–933.
34. Laneville, O.; Breuer, D.K.; Xu, N.; Huang, Z.H.; Gage, D.A.; Watson, J.T.; Lagarde, M.; DeWitt, D.L.; Smith, W.L. Fatty acid substrate specificities of human prostaglandin-endoperoxide H synthase-1 and -2. Formation of 12-hydroxy-(9Z, 13E/Z, 15Z)-octadecatrienoic acids from alpha-linolenic acid. *J. Biol. Chem.* **1995**, *270*, 19330–19336.
35. Liu, W.; Cao, D.; Oh, S.F.; Serhan, C.N.; Kulmacz, R.J. Divergent cyclooxygenase responses to fatty acid structure and peroxide level in fish and mammalian prostaglandin H synthases. *FASEB J.* **2006**, *20*, 1097–1108.
36. Vecchio, A.J.; Simmons, D.M.; Malkowski, M.G. Structural basis of fatty acid substrate binding to cyclooxygenase-2. *J. Biol. Chem.* **2010**, *285*, 22151–22163.
37. Vecchio, A.J.; Orlando, B.J.; Nandagiri, R.; Malkowski, M.G. Investigating substrate promiscuity in cyclooxygenase-2: The role of Arg-120 and residues lining the hydrophobic groove. *J. Biol. Chem.* **2012**, *287*, 24619–24630.
38. Janssen-Timmen, U.; Tomic, I.; Specht, E.; Beilecke, U.; Habenicht, A.J. The arachidonic acid cascade, eicosanoids, and signal transduction. *Ann. N. Y. Acad. Sci.* **1994**, *733*, 325–334.
39. Wensel, S.E. Arachidonic acid metabolites: Mediators of inflammation in asthma. *Pharmacotherapy* **1997**, *17*, 3S–12S.
40. Peng, S.; Okeley, N.M.; Tsai, A.-L.; Wu, G.; Kulmacz, R.J.; van der Donk, W.A. Structural characterization of a pentadienyl radical intermediate formed during catalysis by prostaglandin H synthase-2. *J. Am. Chem. Soc.* **2001**, *123*, 3609–3610.

41. Peng, S.; Okeley, N.M.; Tsai, A.-L.; Wu, G.; Kulmacz, R.J.; van der Donk, W.A. Synthesis of isotopically labeled arachidonic acids to probe the reaction mechanism of prostaglandin H synthase. *J. Am. Chem. Soc.* **2002**, *124*, 10785–10796.
42. Wu, G.; Wei, C.; Kulmacz, R.J.; Osawa, Y.; Tsai, A.-L. A mechanistic study of self-inactivation of the peroxidase activity in prostaglandin H synthase-1. *J. Biol. Chem.* **1999**, *274*, 9231–9237.
43. Wu, G.; Tsai, A.-L.; Kulmacz, R.J. Cyclooxygenase competitive inhibitors alter tyrosyl radical dynamics in prostaglandin h synthase-2. *Biochemistry* **2009**, *48*, 11902–11911.
44. Kulmacz, R.J.; Tsai, A.-L.; Palmer, G. Heme spin states and peroxide-induced radical species in prostaglandin H synthase. *J. Biol. Chem.* **1987**, *262*, 10524–10531.
45. Kulmacz, R.J.; Palmer, G.; Tsai, A.-L. Prostaglandin H synthase: Perturbation of the tyrosyl radical as a probe of anticyclooxygenase agents. *Mol. Pharmacol.* **1991**, *40*, 833–837.

© 2014 by the authors; licensee MDPI, Basel, Switzerland. This article is an open access article distributed under the terms and conditions of the Creative Commons Attribution license (<http://creativecommons.org/licenses/by/3.0/>).